Diffusion and segregation of niobium in fcc-nickel

Damien Connétable, Benoît Ter-Ovanessian, Eric Andrieu

Diffusion and segregation of niobium in fcc-nickel

Damien Connétable, Benoît Ter-Ovanessian and Éric Andrieu

CIRIMAT UMR 5085, CNRS-INP-UPS, École Nationale d'Ingénieurs en Arts Chimiques et Technologiques (ENSIACET) 4, Allée Émile Monso, BP 44362, F-31030 Toulouse Cedex 4, France

E-mail: damien.connetable@ensiacet.fr

Abstract

Niobium is one of the major alloying elements, among the refractory elements, contributing to the strengthening of superalloys. Consequently, data about its behavior and its migration mechanism in fcc-Ni are essential knowledge to understand and control the strengthening in such alloys. We present in this work Nb interactions, solubility and diffusion in Ni performed by using the GGA approximation of the density functional theory. The substituted site is found to be the most favorable configuration in comparison to the tetrahedral and octahedral sites. The effect of temperature on solubility is discussed taking into account the thermal expansion of the lattice parameter and the vibrational contribution. Its diffusion mechanism is also discussed and compared to the literature. We finally discuss the segregation of Nb atoms on a Σ_5-(012) symmetric tilt grain boundary.

1. Introduction

Refractory elements are considered as key alloying elements in Ni-based superalloys because they lead to the improvement of the superalloys' mechanical properties and behavior at low and high temperatures [1–3]. Among the refractory elements, niobium is one of the major alloying elements contributing to the strengthening of superalloys, especially for precipitation-hardened Ni-based superalloys such as alloys 706, 718, 725 and more [4, 5]. Indeed, niobium contributes not only to solid solution strengthening, strengthening through carbide formation, but also to precipitation hardening, sometimes by improvement of the γ'-phase Ni_3Al properties and essentially by the formation of γ''-phase Ni_3Nb during aging treatment [4–6]. The γ'' phase is commonly considered as the principal location of the niobium and as primarily responsible for the strengthening mechanism [4–7]. Consequently, good mechanical properties, generally attributed to the coherency strains between γ'' and the matrix (γ) [7], are mainly controlled by γ'' precipitate particle size and distribution. Precipitation and coarsening behaviors of γ'' phase have been reported to be mainly due to initial segregation resulting from elaboration processes [8] and volume diffusion of niobium in the matrix [9].

Therefore, the knowledge of niobium diffusion and niobium interactions in nickel matrix seems to be a requirement in order to improve the understanding of the strengthening mechanism of such alloys. Accordingly, in the present study, an *ab initio* study of interactions between Nb and Ni atoms was performed. Firstly, the configuration of one Nb atom in solution in the γ matrix was studied: in substitution configuration as well as in insertion configuration. Secondly, the influences of temperature and of neighborhood on these configurations were examined. Finally, regarding the obtained results, Nb diffusion and segregation processes were discussed. For instance, the segregation energy of a Nb atom on a Σ_5-(012) grain boundary was calculated and discussed.

2. Computational details

Calculations were done within the density functional theory formalism (DFT) and the pseudopotential approximation. They were performed by means of plane wave methods as implemented in the Vienna *ab initio* simulation program (VASP) [10]. Projected augmented wave pseudopotentials (PAW) [11], and the Perdew–Wang generalized gradient approximation (GGA) [12] of the exchange and correlation functional within its spin-polarized version were used. The

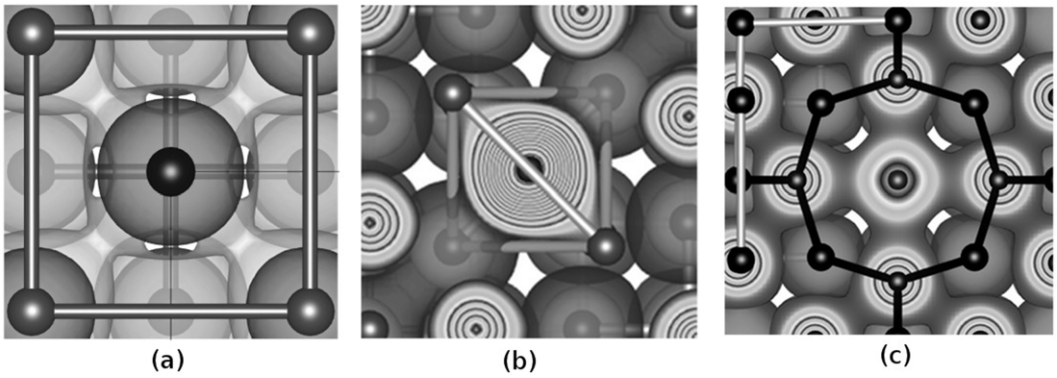

Figure 1. Representation of the electron charge density of niobium in fcc-Ni: Nb in substitution (a), tetrahedral (b) and octahedral sites (c). We have underlined in black Ni–Ni bonds.

cut-off was fixed to 400 eV for calculations. Dense mesh grids equivalent to a 24 × 24 × 24 **k**-mesh grid for a unit cell with one atom (a band folding approach is used for supercells) were used. These criteria allow us to check a good convergence (<1 meV/atom). Lattice relaxation, introduced by using a conjugate gradient algorithm, was taken into account. All ions and defects were allowed to relax.

Preliminarily pseudopotentials of both elements were tested. As previously published for Ni, the pseudopotential reproduces satisfactory the main properties of the Ni-fcc phase (γ): cohesive energy, lattice parameters, and elastic properties (see [13]). For Nb in a bcc phase, the cohesive energy is found to be equal to about 7.09 eV (experiment 7.57 eV [14]), for a lattice parameter equal to 3.32 Å (experiment 3.30 Å [14]). We also test them in Ni–Nb binary configurations (not presented here). Our results are in good agreement with the ones obtained within the PBE functional [15, 16], which convinces us of the accuracy of the pseudopotentials.

3. Nb in solution

To study the influence of Nb in solution in γ, three possible configurations were considered: the substitution site and the two insertion sites (tetrahedral and octahedral, labeled T and O, respectively). To quantify the relative stability of one site in comparison to another, two energies are defined: the insertion (E_{ins}) and solubility (E_{sol}) energies.

In the case of insertion (T and O), $E^{\mathrm{T/O}}_{\mathrm{ins/sol}}$ are defined by

$$E^{\mathrm{T/O}}_{\mathrm{ins/sol}}[\mathrm{Nb}] = E[n\mathrm{Ni} + \mathrm{Nb}] - E[n\mathrm{Ni}] - E_{\mathrm{a/r}}[\mathrm{Nb}] \quad (1)$$

where $E_{\mathrm{a}}[\mathrm{Nb}]$ and $E_{\mathrm{r}}[\mathrm{Nb}]$ correspond to the energy of a Nb atom and the energy of the Nb reference state (bcc-Nb), respectively. $E[n\mathrm{Ni}]$ is the total energy of the supercell containing n atoms of Ni. In the case of substitution, an equivalent expression may be used:

$$E^{\mathrm{S}}_{\mathrm{ins/sol}}[\mathrm{Nb}] = E[(n-1)\mathrm{Ni} + \mathrm{Nb}] - \frac{n-1}{n}E[n\mathrm{Ni}] - E_{\mathrm{a/r}}[\mathrm{Nb}]. \quad (2)$$

These energies, as a function of the size of the supercell, are listed in table 1. The first finding is that the Nb atom prefers to be in substitution, in agreement with experimental hypothesis [21]. Indeed, due to its large size (the covalent radii of Nb and Ni are equal to 1.46 and 1.24 Å, respectively) and its shells ($5s^2 4d^3$ configuration), Nb atoms are assumed to prefer the substitution sites. Besides, for this configuration, we show that the effect of the relaxation of the lattice parameter fast became negligible (2 × 2 × 2 supercells gives equivalent results to 4 × 4 × 4 supercells). The solubility and the insertion energies in substitution are both found to be negative: −0.66 and −7.75 eV, respectively.

These results (the evolution of the energies with respect to the supercell) also show that the Nb–Nb interactions are short range. The stress field induced by the substitution is short range. In the literature, neither the energy of insertion, nor the solubility of the Nb atom, is reported, thus making the comparison with experimental data difficult. The zero point energy (vibrational free energy) in substitution (computed on a 2 × 2 × 2 supercell at the Γ point) is found to modify the energies slightly: about 15 and 11 meV for the insertion and solubility vibrational free energies respectively (without and with the bcc-Nb contribution, respectively[1]).

The energies of tetrahedral and octahedral sites are found to be positive and equivalent. In the case of the insertion sites, the relaxation of the Ni first nearest neighboring atoms is large even with large supercells (4×4×4), which explains the strong positive energy of the solubility (+4.23 and +4.26 eV, for T and O respectively). Long range deformations are due mainly to the steric effects (see figure 1).

In addition to the former results, the nature of bonds between Nb and Ni atoms using the charge transfer and the electron density of charge around the impurity were analyzed. As the results above suggest, the effect of Nb in substitution on the electron density is slight; the steric effects are low. The charge transfer between the Nb atom and the surrounding Ni (Bader's charges [18]) indicates that the net charge on Nb is close to around −1.2 electron for the substitutional site. Nb is thus slightly anionic. Its electronic environment, displayed in figure 1, becomes closer to that of nickel. In tetrahedral sites, the charge transfer is found to be equal to that in substitution (−1.2 electron), while in octahedral sites it is smaller (−0.4 electron).

[1] Computed on a 4 × 4 × 4 q-grid, 40 Ryd and 20 × 20 × 20 k-mesh [17].

Table 1. Insertion (E_{ins}, in eV) and solubility (E_{sol}, in eV) energies of niobium in substitution and tetrahedral and octahedral interstitial positions, for different lattice parameters and supercells.

	$2 \times 2 \times 2$			$3 \times 3 \times 3$		$4 \times 4 \times 4$	
Supercell	E_{sol}	E_{ins}	F_{vib}	E_{sol}	E_{ins}	E_{sol}	E_{ins}
			$a_o = 3.52$ Å ($T = 0$ K)				
Nb_{sub}	−0.61/−0.67[a]	−7.69/−7.75[a]	−0.021	−0.66/−0.66[a]	−7.74/−7.75[a]	−0.67	−7.76
Nb_{tetra}	6.22/4.71[a]	−0.86/−2.38[a]	—	4.72/4.23[a]	−2.37/−2.85[a]	4.48	−2.61/−2.86
Nb_{octa}	4.93/4.29[a]	−2.16/−2.79[a]	—	4.63/4.26[a]	−2.46/−2.83[a]	4.45	−2.64/−2.80
			$a_o = 3.56$ Å ($T = 890$ K)				
Nb_{sub}	−0.87	−7.96	+0.310	−0.92	−8.00	−0.92	−8.01
			$a_o = 3.60$ Å ($T = 1450$ K)				
Nb_{sub}	−1.09	−8.17	+0.555	−1.12	−8.21	−1.13	−8.22

[a] Unrelaxed/relaxed unit cell.

4. Effect of temperature

Furthermore, we have studied the effect of temperature on the substitution energies. For such study, a practical approach has been developed in order to include in our simulations some empirical parameters, from literature or theoretical results. In the present work, experimental data of the thermal expansion of the fcc-Ni lattice parameter are taken into account (see [19] for details). We fix the volume to that of the empirical parameters, and all calculations are done for this value. A similar approach has already been used successfully in the study of the diffusion of hydrogen in fcc-Ni [20]. At a given T, the free energy of the system is given by

$$F(T) = F[(n-1)\mathrm{Ni} + \mathrm{Nb}](V_1(T)) - \frac{n-1}{n} F[n\mathrm{Ni}](V_2(T)) - F_{\mathrm{ref}}[\mathrm{Nb}](V_3(T)). \quad (3)$$

We neglect the effect of insertion of niobium on the lattice parameter (V, volume of the cell) of Ni-fcc ($V_1 = V_2$). The volume of the cell is dependent on the temperature by means of the thermal expansion of the lattice parameters given by Wimmer (see equation (3), [20]). For the reference state, we have used the experimental lattice expansion of bcc-Nb. In each configuration, the vibrational contribution is taken into account. Results are reported in the table 1.

We note that the effect of temperature results in a decrease of the internal energy, whereas the vibrational contribution increases. To enlarge our analysis of insertion energies, we have computed the vibrational contribution of Nb-bcc, calculated at the experimental volume for a given T. At 0 K, we find a small correction (+4 meV/atom), which decreases rapidly to become significant negative values: the correction is about −363 and −787 meV/atom at 890 K and 1450 K, respectively. This suggests that the solubility energy is strongly affected by the temperature and the main contribution is due to the vibrational part.

5. Multi-defect interactions: V–Nb and Nb–Nb

In a second step, we have analyzed the interactions of a Nb atom in substitution with another impurity: either a vacancy or another Nb atom. The binding energies between Nb and X (X = V or Nb) defined as

$$E_b[\mathrm{Nb, X}] = (E[(n-2)\mathrm{Ni, Nb, X}] + E[n\mathrm{Ni}]) - (E[(n-1)\mathrm{Ni, Nb}] + E[(n-1)\mathrm{Ni, X}]) \quad (4)$$

are presented in table 2 as a function of the distance of Nb from the second defect X. We restrict ourselves to the first (1NN) up to the fourth nearest neighboring configurations (4NN). With our convention, a negative energy is associated with an attractive interaction. In the first neighboring configuration, it is worth noticing that Nb–Nb interactions are strongly repulsive (+0.5 eV) and are rapidly decreasing (up to the 3NN configuration). These results are in agreement with our previous analysis.

Table 2. Formation (E_f, in eV) and binding energies (E_b, in eV) of the Nb–X defect (X = vacancy or Nb), as a function of the distances (d(Nb–X), in Å) of each elementary defect.

	d(Nb–X)	Nb–V E_b	Nb–Nb E_b
1NN	2.49 ($a_o/\sqrt{2}$)	−0.13	0.52
2NN	3.52 (a_o)	0.04	0.19
3NN	4.31 ($a_o\sqrt{3/2}$)	−0.01	−0.07
4NN	4.98 ($a_o\sqrt{2}$)	−0.08	−0.01

These data suggest that Nb atoms prefer to interact with Ni atoms rather than to be in bcc-Nb. If we compare these results with formation energies of Ni–Nb binaries (computed with an equivalent approach [16]), we note that the solubility energy is twice as large as for the Ni_3Nb–$D0_{22}$ system (around −300 meV/atom), which suggests that Nb–Nb interactions are not favored in solution.

In the case of interactions of a Nb and a vacancy, it is worth mentioning that 1NN is an attractive configuration (around −130 meV). The vacancies in the 2NN configurations are slightly repulsive, but the trend is an attractive interaction with the vacancy (4NN). These results suggest that Nb should trap vacancies.

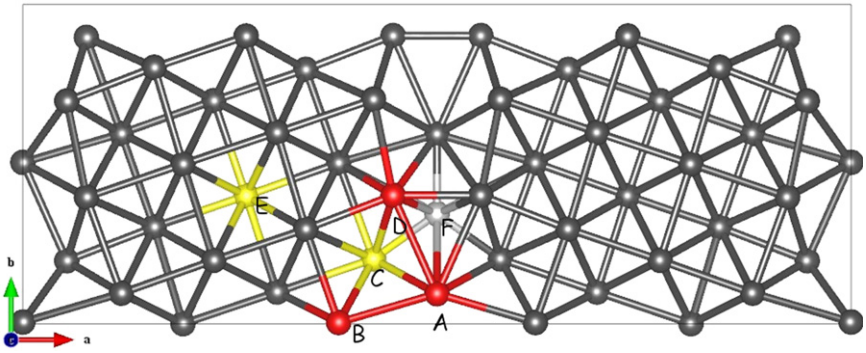

Figure 2. Schematic representation of the Σ_5-(012) grain boundary. In red and yellow, we have underlined the different configurations studied. Yellow and red atoms are located in two different planes. In gray, we represent the open site; this site is empty site except in the F configuration.

Table 3. Migration, formation and activation energies (in eV) for different temperatures.

T (K)	a_o (Å)	H^f_{1v}	H^m	H^a
0	3.52	1.41/1.43[a]	0.66	2.07/2.09[a]
890	3.56	1.58/1.65[a]	0.66	2.13/2.20[a]
1450	3.60	1.65/1.84[a]	0.67	2.23/2.42[a]

[a] Without/with vibrational contribution.

Table 4. Segregation energy (E_{seg}[Nb], in eV) of a Nb atom on the Σ_5-(012) grain boundary.

Configuration	E_{seg}[Nb]	Configuration	E_{seg}[Nb]
A	−1.11	D	−0.61
B	−0.66	E = bulk	−0.58
C	−1.01	F = opensite	+0.56

6. Diffusion of niobium

The diffusion process of the Nb atom was also investigated. Experimentally, Patil and Karunaratne studied the chemical diffusion of Nb atoms in Ni [21, 22]. They measured the diffusion coefficient at high temperature (900–1400 K), and described it from an Arrhenius curve type: $D_{Nb} = D_o \exp(-\frac{H^a}{RT})$ with $H^a = 202.59 \pm 4.71$ kJ mol^{-1} $\simeq$ 2.10 eV and $D_o = 1.04^{+0.87}_{-0.48} \times 10^{-6}$ m^2 s^{-1} for Patil [21] and $H^a = 257.0$ kJ mol^{-1} $\simeq$ 2.66 eV and $D_o = 8.8^{+3.2}_{-2.3} \times 10^{-5}$ m^2 s^{-1} for Karunaratne [22]. The diffusion mechanism of Nb atoms is found to be slow in nickel. In a first approximation, we model the migration mechanism of Nb atoms as $D_o C_{1v} \exp(-H^m/k_B T)$, where C_{1v} is the concentration of monovacancies, and H^m the migration energy of Nb through the vacancy. C_{1v} is defined by

$$C_{1v} = \exp\left[\frac{S^f_{1v}}{k_B}\right] \exp\left[-\frac{H^f_{1v}}{k_B T}\right] \quad (5)$$

where H^f_{1v} is the formation energy of the monovacancy.

Our results are summarized in table 3. In this part of the study, the effects of temperature are taken into account thank to the procedure previously described. The formation energies of the monovacancy are reported with and without vibrational contribution of the enthalpy energy. The final migration energy is evaluated to be about 2.1 eV, in excellent agreement with experimental data. The effect of temperature on migration energies is evaluated on only the first migration path (H^m). The migration energy of Nb atoms is small depending of the effect of the dilatation of the lattice: about 0.66 eV. The main evolution is due to the formation energy of the vacancy. With this correction and the vibrational contribution, we notice that at high temperatures the activation energy tends to the value of Karunaratne.

7. Segregation on a Σ_5-(012) grain boundary

The segregation of a Nb atom on the Ni Σ_5-(012) symmetrical tilt grain boundary is finally discussed. The grain boundary used is the same as presented by Yamaguchi [23] (see figure 2). There are two grain boundaries per unit cell. Along the z direction four interatomic planes between Nb atoms are introduced to reduce Nb–Nb interactions. For the undoped grain boundary, the excess surface energy γ_{gb} is found to be equal to about 1.25 J m^{-2}, in agreement with previous theoretical works (1.43 J m^{-2} [23]). We considered six different configurations to place Nb: in A–D near the grain boundary, in the open site E, and in the open site F (see figure 2). The segregation energy is defined as (except for the F configuration, where the factor $(n-1)/n$ disappears)

$$E_{seg}[\mathrm{Nb}] = E_{gb}[(n-1)\mathrm{Ni} + \mathrm{Nb}] - \frac{n-1}{n} E_{gb}[n\mathrm{Ni}] - E_{ref}[\mathrm{Nb}]. \quad (6)$$

Segregation energies (E_{seg}[Nb]) are reported in table 4 and can be compared to results in the bulk. We note that Nb atoms segregate easily on the grain boundaries. E_{seg}[Nb] is even twice that in the bulk. In cases B, D and F, the energies correspond to the energy in the grain. Case E leads to a counter-intuitive result. It is not a stable configuration for Nb atoms.

These results show that Nb atoms are more likely located near grain boundaries than in the bulk. They are correlated to the experimental results where Nb atoms modify the mobility of the interfaces [24, 8, 25].

8. Conclusion

To conclude, we have further explored the behavior of the Nb atom impurity in fcc-Ni. We show that, as in experimental findings, Nb atoms prefer to be located in the substitutional sites. We evaluate their solubility to be about -0.66 eV at low temperature. The chemical similitude between Nb and Ni atoms is the main explanation for their good miscibility in the network. We show that vacancies are attracted by Nb, but the low concentration of vacancies in Ni induces a low diffusion in the material. The theoretical activation energy is found to be in agreement with experimental data. The main contribution is due to the formation energy of the monovacancy. Finally, the study of Nb segregation on a Σ_5-(012) grain boundary shows that the segregation of Nb atoms is easier than in the bulk, suggesting that the Nb segregates easily on these interfaces. This segregation should play a significant role in the repartition of mechanical properties in alloys.

Acknowledgments

This work was granted access to the HPC resources of CALMIP (CICT Toulouse, France) under the allocations 2009/2010-p0842 and 2011-p0912. DC thanks D Monceau for fruitful discussions, and C Marquier for help on the grain boundaries. Figures were drawn using the `VESTA` package [26].

References

[1] Sims C T 1984 *Proc. Superalloys* TMS, p 399
[2] Jena A K and Chaturvedi M C 1984 *J. Mater. Sci.* **19** 3121
[3] Sabol G P and Stickler R 1969 *Phys. Status Solidi* **39** 11
[4] Smith G D and Patel S J 2005 *Proc. Superalloys 718, 625, 706 And Various Derivatives* TMS, p 135
[5] Guo E and Ma F 1980 *Proc. Superalloys* TMS, p 431
[6] Paulonis D F, Oblak J M and Duvall D S 1969 *ASM Trans.* **62** 611
[7] Oblak J M, Paulonis D F and Duvall D S 1974 *Metall. Trans.* **5** 143
[8] Dong Y W, Jiang Z H and Li Z B 2009 *J. Iron Steel Res.* **16** 7
[9] Devaux A, Nazé L, Molins R, Pineau A, Organista A, Guédou J Y, Uginet J F and Héritier P 2008 *Mater. Sci. Eng.* A **486** 117
[10] Kresse G and Hafner J 1993 *Phys. Rev.* B **47** 558
Kresse G and Hafner J 1994 *Phys. Rev.* B **49** 14251
Kresse G and Furthmüller J 1996 *Phys. Rev.* B **54** 11169
Kresse G and Furthmüller J 1996 *Comput. Mater. Sci.* **6** 15
[11] Kresse G and Joubert D 1999 *Phys. Rev.* B **59** 1758
[12] Wang Y and Perdew J P 1991 *Phys. Rev.* B **44** 13298
[13] Connétable D and Thomas O 2009 *Phys. Rev.* B **79** 094101
[14] Kittel C 1996 *Introduction to Solid State Physics* (New York: Wiley)
[15] Perdew J P, Burke K and Ernzerhof M 1996 *Phys. Rev. Lett.* **77** 3865
Perdew J P, Burke K and Ernzerhof M 1997 *Phys. Rev. Lett.* **78** 1396
[16] Connétable D, Mathon M and Lacaze J 2011 *Calphad Computer Coupling of Phase Diagrams and Thermochemistry* **35** 588–93
[17] Giannozzi P *et al* 2009 *J. Phys.: Condens. Matter* **21** 395502
[18] Henkelman G, Arnaldsson A and Jónsson H 2006 *Comput. Mater. Sci.* **36** 354
[19] Connétable D, Ter Ovanessian B, Monceau D and Andrieu E 2012 submitted
[20] Wimmer E, Wolf W, Sticht J, Saxe P, Geller C B, Najafabadi R and Young G A 2008 *Phys. Rev.* B **77** 134305
[21] Patil R V and Kale G B 1996 *J. Nucl. Mater.* **230** 57
[22] Karunaratne M S A and Reed R C 2005 *Defect Diffus. Forum* **237–240** 420
[23] Yamaguchi M, Shiga M and Kaburaki H 2004 *J. Phys.: Condens. Matter* **16** 3933
[24] Muratov L S and Cooper B R 1998 *J. Phase Equilib.* **19** 503–12
[25] Pang X J, Dwyer D J, Gao M, Valerio P and Wei R P 1994 *Scr. Metall. Mater.* **31** 345–50
[26] Momma K and Izumi F 2008 *J. Appl. Crystallogr.* **41** 653–8